doi:10.3772/j.issn.1006-6748.2019.04.014

Coordination control for crankshaft forging hydraulic press①

Yao Jing(姚 静)②*,**,***, Li Yao*, Cao Xiaoming*, Sha Tong*
(* College of Mechanical Engineering, Yanshan University, Qinhuangdao 066004, P. R. China)
(** The Laboratory of Heavy Machinery Fluid Power Transmission and Control in Hebei, Yanshan University, Qinhuangdao 066004, P. R. China)
(*** The State Key Laboratory of Fluid Power and Mechatronic Systems, Zhejiang University, Hangzhou 310058, P. R. China)

Abstract

Taking a new type of full-fiber crankshaft forging hydraulic press as the research object, an upsetting-bending stroke coordination control is studied to improve crankshaft forming accuracy. A master-slave proportion integration differentiation (PID) coordination control strategy based on velocity feed-forward is proposed to improve the coordination control accuracy. The structure and working process of the full-fiber crankshaft forging hydraulic press are introduced, and a mathematical model of the upsetting and bending control system are established. The coordination control strategy is verified experimentally. The experimental results show that the maximum tracking error of the coordination control strategy is reduced by 66% compared with the traditional PID controller, and the coordination motion accuracy is improved effectively.

Key words: crankshaft forging hydraulic press, coordination control, velocity feed-forward, master-slave proportion integration differentiation (PID) control

0 Introduction

A crankshaft is a key component of ship and automobile engines. Good mechanical property and high reliability of full-fiber crankshafts are crucial to the smoothness and safety on the operation of ships and automobiles[1]. So far, large-scale full-fiber crankshafts are generally made by forging on a large-scale hydraulic press with a special die in China[2,3]. The crankshaft forged by this method has the problems of high cost, complicated process, low efficiency, and destruction of metal flow lines, which affect the mechanical property and service life of the crankshaft. Therefore, many scholars have devoted to the study of new processes and new equipment for crankshaft manufacturing. Based on TR method, the new TR method (NTR) controls the bending cylinder individually to adjust the upsetting and bending process parameters separately to further improve the quality of the crankshaft[4-6].

The upsetting-bending forging method is a 2-way forging method. The forging is subjected to upsetting and shear force simultaneously, and finally forged into a crankshaft. If the upsetting and bending processes are not coordinated, the crankshaft is prone to produce defects such as ‘missing angle’ or other poor filling performance[7], which affects the overall quality and forming accuracy of the crankshaft. In order to improve the forming accuracy of the crankshaft forging hydraulic press, one of the key technologies is the coordination control of the upsetting cylinder-bending cylinder.

The existing researches focus on the synchronous control of multi-cylinder[8-17], and few researches have been performed on coordination control methods of multi-cylinder. Based on the characteristics of upsetting-bending coordination process of NTR method, a master-slave proportion integration differentiation (PID) coordination control strategy is designed based on velocity feed-forward, which is applied to the upsetting cylinder-bending cylinder coordination control system and verified by experiments.

1 Configuration of NTR

1.1 Structure of upsetting-bending hydraulic press

① Supported by the National Natural Science Foundation of China (No. 51575471), Natural Science Foundation of Hebei Province (No. E2018203028), Open Foundation of the State Key Laboratory of Fluid Power and Mechatronic Systems (No. GZKF-201716), the Key Project of Science and Technology Plan of Higher Education of Hebei Education Department (No. ZD2017077) and National Basic Research Program of China (No. 2014CB046405).
② To whom correspondence should be addressed. E-mail: jyao@ysu.edu.cn
Received on Oct. 20, 2018

The principle of bending and upsetting for full-fiber crankshaft by NTR method is studied in this paper. The body structure of the full-fiber crankshaft forging hydraulic press is shown in Fig. 1.

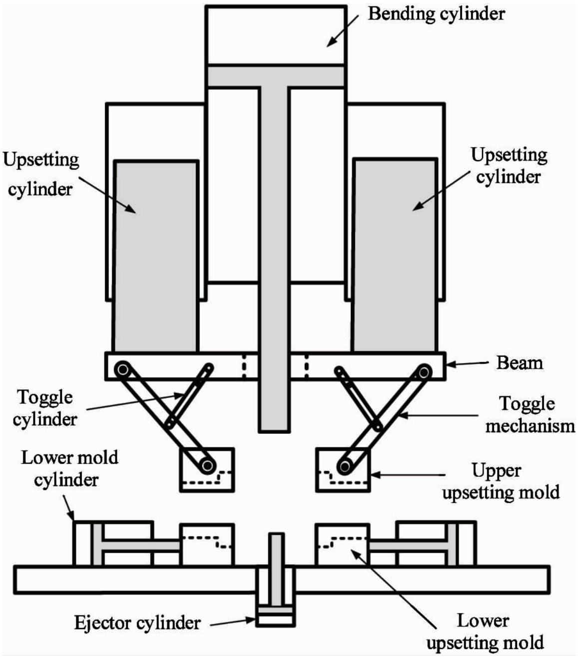

Fig. 1 Structure of upsetting-bending hydraulic press diagram

The hydraulic press consists of an upsetting system for crankshaft upsetting and a bending system for forming crank. The upsetting system consists of 2 upsetting cylinders (Plunger cylinder), beam, toggle mechanism, toggle cylinder, lower mold cylinder, upper upsetting mold and lower upsetting mold. Two upsetting cylinders are hinged with the beam. One end of toggle mechanism is hinged with the beam, the other end is hinged with the upper upsetting mold.

The bending system consists of the bending cylinder (piston cylinder), ejector cylinder and bending mold.

During the forming process of the crankshaft, the upsetting system drives the beam downward. The downward driving force of the upsetting cylinder is converted into the horizontal force of the upsetting mold by the toggle mechanism, and the upsetting process of the crankshaft is completed by the movement of upsetting mold toward each other.

The bending cylinder independently drives the bending mold to form the crank of crankshaft.

The upsetting system and the bending system coordinate with each other according to the determined crankshaft forming process. Finally the full-fiber crankshaft with high accuracy and good mechanical properties can be formed. Furthermore, different types of the full-fiber crankshaft can be formed by adjusting the parameters of upsetting-bending coordination process.

1.2 Upsetting-bending coordination process

Upsetting-bending forming phase 1. The upsetting cylinder drives the beam downward, and the beam drives the upsetting mold to move towards each other through the toggle mechanism. The bending cylinder moves with a given upsetting-bending stroke which is shown in Fig. 2.

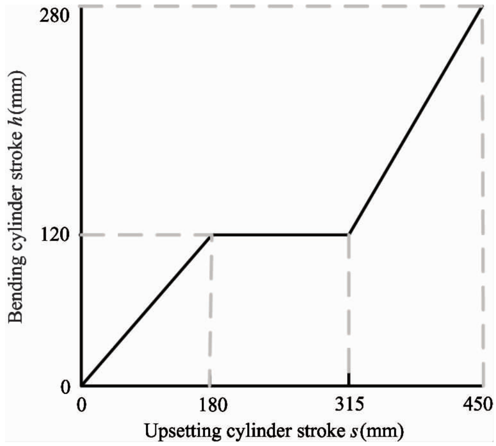

Fig. 2 Upsetting-bending coordination motion curve

Upsetting-bending forming phase 2. The upsetting cylinder continues to keep synchronous motion at a certain speed for the upsetting of the crankshaft. Meanwhile, the bending cylinder keeps a certain output force.

Upsetting-bending forming phase 3. The upsetting cylinder continues to drive the upsetting mold, and the bending cylinder continues to move according to a given upsetting-bending stroke in order to ensure the final forging accuracy.

2 System modelling

2.1 Upsetting system mathematical model

In order to facilitate the establishment of a mathematical model, the necessary simplification of the upsetting system is carried out without affecting the characteristics of the upsetting synchronous control system:

1) Setting the beam as a rigid body and neglecting the thickness of the moving beam.

2) No translation activities of the beam in the horizontal plane.

3) The deflection angle of the beam is very small.

The simplified model of the upsetting cylinder control system is shown in Fig. 3.

Based on the above assumptions, the relationship between the 2 cylinders' displacements and the movement of the moving beam are shown as follows:

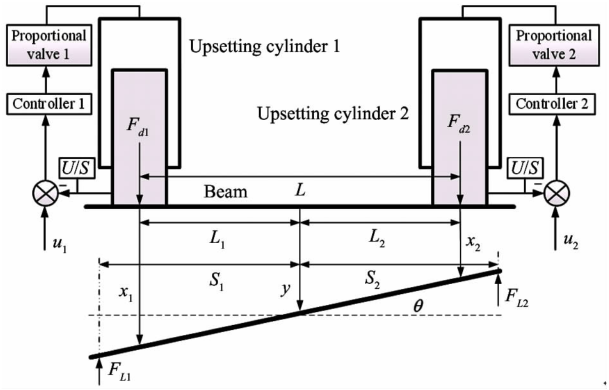

Fig. 3 Simplified model of upsetting cylinder control system

$$\begin{cases} \theta = \dfrac{x_2 - x_1}{L} \\ y = \dfrac{L_1 x_1 + L_2 x_2}{L} \end{cases} \tag{1}$$

where, θ is the deflection angle of the beam (rad), L is the distance between 2 upsetting cylinders (m), y is centroid displacement of the moving beam (m), x_1 and x_2 are 2 upsetting cylinders displacement respectively (m), L_1 and L_2 are the distances from the centroid to the 2 cylinders (m).

The dynamic equation of the beam is:

$$\begin{cases} F_{d1} + F_{d2} + Mg - F_{L1} - F_{L2} = M\dfrac{\mathrm{d}^2 y}{\mathrm{d}t^2} \\ F_{d1}L_1 - F_{d2}L_2 + F_{L2}S_2 - F_{L1}S_1 = J\dfrac{\mathrm{d}^2\theta}{\mathrm{d}t^2} \end{cases} \tag{2}$$

where, F_{d1} and F_{d2} are output forces of 2 upsetting cylinders (N), F_{L1} and F_{L2} are the load forces acting on the 2 positions of the beam (N), S_1 and S_2 are the distances from the centroid to the load acting point on the beam (m), M is the mass of the beam (kg), J is the rotational inertia of the beam (kg · m^2).

The flow equations through 2 electro-hydraulic proportional valves can be expressed as:

$$\begin{cases} Q_1 = C_{d1}\omega x_{v1}\sqrt{\dfrac{2(p_s - p_1)}{\rho}} \\ Q_2 = C_{d2}\omega x_{v2}\sqrt{\dfrac{2(p_s - p_2)}{\rho}} \end{cases} \tag{3}$$

where, Q_1 and Q_2 are the flows of 2 upsetting cylinders respectively (L/min), x_{v1} and x_{v2} are the spool displacements of 2 electro-hydraulic proportional valves respectively (m), C_{d1} and C_{d2} are flow rate coefficients, p_1 and p_2 are the pressures of the electro-hydraulic proportional valve (MPa), ω is the cross-section grads of the electro-hydraulic proportional valves (m), and p_s is the supply pressure (MPa).

The flow rate continuity equations of the 2 upsetting cylinders are:

$$\begin{cases} Q_1 = \dfrac{\mathrm{d}V_1}{\mathrm{d}t} + \dfrac{V_1}{\beta_e}\dot{p}_1 + C_{ep1}p_1 \Rightarrow \dot{p}_1 = \dfrac{\beta_e}{V_1}(Q_1 - A_1\dot{x}_1 - C_{ep1}p_1) \\ Q_2 = \dfrac{\mathrm{d}V_2}{\mathrm{d}t} + \dfrac{V_2}{\beta_e}\dot{p}_2 + C_{ep2}p_2 \Rightarrow \dot{p}_2 = \dfrac{\beta_e}{V_2}(Q_2 - A_2\dot{x}_2 - C_{ep1}p_2) \end{cases} \tag{4}$$

where, V_1 and V_2 are the compressed volumes of the 2 upsetting cylinders respectively (m^3), C_{ep1} and C_{ep2} are the coefficients of the external leakage of the 2 upsetting cylinders respectively (m^3/(Pa · s)), A_1 and A_2 are the effective acting area of the 2 upsetting cylinders' pistons respectively (m^2) and β_e is the effective bulk modulus of oil (Pa).

The force balance equations for the 2 upsetting cylinders are:

$$\begin{cases} m_1\ddot{x}_1 = p_1A_1 + m_1 g - F_{d1} - B_{p1}\dot{x}_1 - f_1 \\ m_2\ddot{x}_2 = p_2A_2 + m_2 g - F_{d2} - B_{p2}\dot{x}_2 - f_2 \end{cases} \tag{5}$$

where, m_1 and m_2 are the piston masses of the 2 upsetting cylinders (kg), B_{p1} and B_{p2} are viscous damping coefficients of the 2 upsetting cylinders respectively ((N · s)/m) and f_1 and f_2 are frictions of the 2 upsetting cylinders respectively (N).

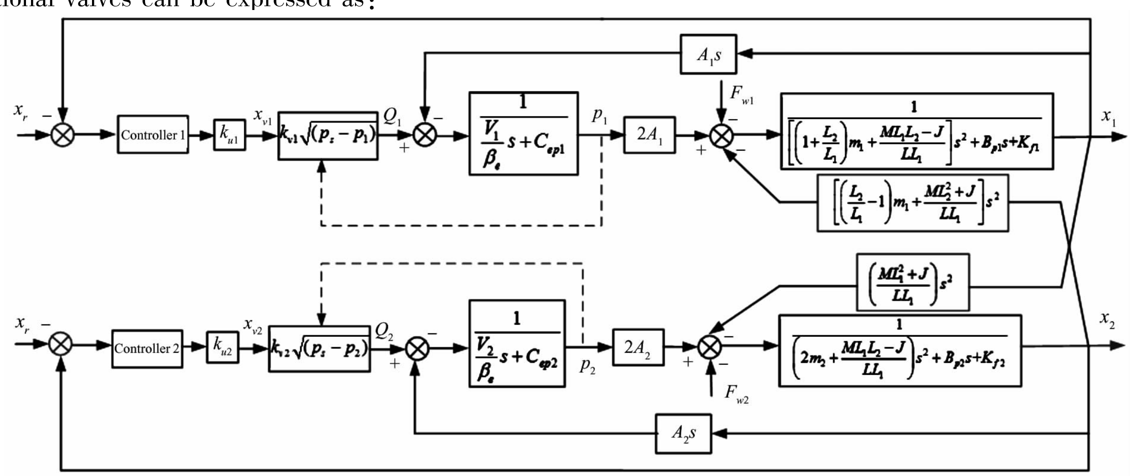

Fig. 4 Upsetting control system block diagram

After the Laplace transform, the block diagram of the upsetting control system is shown in Fig. 4.

2.2 Bending system mathematical model

The bending cylinder is used to form the crank-throw of the crankshaft which is coordinated with the upsetting cylinder. The bending cylinder is controlled independently and its control principle can be regarded as a zero lap 4-way slide valve control asymmetric cylinder system. Simplified model of the bending cylinder control system is shown in Fig. 5.

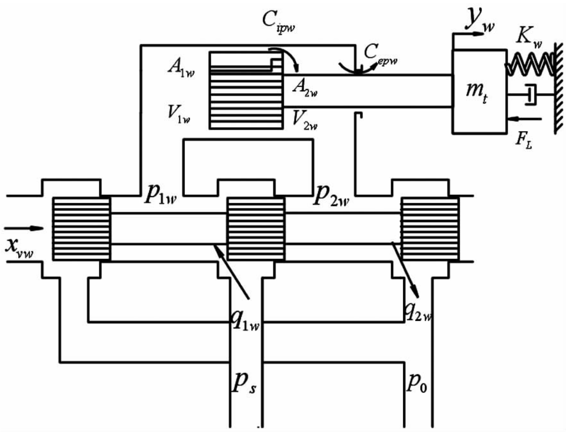

Fig. 5 Simplified model of bending cylinder control system

When $\dot{y}_w > 0$, the spool of proportional valve moves to the right to drive bending cylinder piston out, namely, $x_{vw} > 0$.

The necessary simplification of the upsetting system is carried out:

1) The proportional valve is a zero lap 4-way slide valve.

2) The 4 throttle windows are symmetrical.

3) The supply pressure p_s is constant.

4) The return pressure p_0 is zero.

Flow equation of the electro-hydraulic proportional valve can be expressed as

$$\begin{cases} q_{1w} = C_{dw}\omega x_{vw}\sqrt{\dfrac{2}{\rho}(p_s - p_{1w})} \approx A_{1w}\dot{y}_w \\ q_{2w} = C_{dw}\omega x_{vw}\sqrt{\dfrac{2}{\rho}(p_{2w} - p_0)} \approx A_{2w}\dot{y}_w \end{cases} \tag{6}$$

where, q_{1w} and q_{2w} are the flows of rodless cavity and rod cavity respectively (L/min), x_{vw} is the spool displacement of electro-hydraulic proportional valve (m), C_{dw} is the flow rate coefficient of electro-hydraulic proportional valves , A_{1w} and A_{2w} are the effective acting areas of rodless cavity and rod cavity respectively (m^2), p_{1w} and p_{2w} are the pressures of rodless cavity and rod cavity respectively (MPa), ω is the cross-section grads of the electro-hydraulic proportional valve (m), p_s is the supply pressure (MPa), p_0 is the return pressure (MPa) and y_w is the displacement of the bending cylinder piston (m).

The load flow of the asymmetric cylinder is defined:

$$q_L = \frac{q_{1w} + nq_{2w}}{1 + n^2} \tag{7}$$

It can be known from the equation of flow continuity of an asymmetric hydraulic cylinder's 2 chambers:

$$q_{2w} = nq_{1w} \tag{8}$$

Therefore, when the system is static, the load flow satisfies Eq. (9).

$$q_L = q_{1w} \tag{9}$$

Therefore, the load flow of the bending system is described by the flow of the asymmetric cylinder's rodless cavity. That is, the flow continuity equation of the bending cylinder is:

$$\begin{cases} q_L = C'_{ip}p_L - C_f p_s + \dfrac{V_t}{4\beta_e}\dot{p}_L + A_{1w}\dot{y}_w \\ C'_{ip} = \dfrac{(1 + n^2)C_{ipw}}{1 + n^3},\ C_f = \dfrac{n^2(1 - n)C_{ipw}}{1 + n^3}, \\ \qquad V_t = \dfrac{4V_{1w}}{1 + n^3} \end{cases} \tag{10}$$

where, C_{ipw} is the internal leakage coefficient of the bending cylinder ($m^3/(Pa \cdot s)$), C'_{ip} is the equivalent leakage coefficient of the bending cylinder ($m^3/(Pa \cdot s)$), C_f is the additional leakage coefficient of the bending cylinder ($m^3/(Pa \cdot s)$), V_t is the equivalent volume of the bending cylinder (m^3). Take $V_{1w} = \dfrac{L'A_{1w}}{2}$, then $V_t = \dfrac{2L'A_{1w}}{(1 + n^3)}$, where, L' is the total stroke of the bending cylinder (m).

The force balance equation of the bending cylinder is:

$$\begin{aligned} p_{1w}A_{1w} - p_{2w}A_{2w} &= p_L A_{1w} \\ &= m_w\ddot{y}_w + B_{pw}\dot{y}_w + K_w y_w + F_L \end{aligned} \tag{11}$$

where, m_w is the equivalent mass of the bending cylinder's piston and load (kg), B_{pw} is viscous damping coefficient of the bending cylinder ((N · s)/m), K_w is the elastic stiffness of the bending load, (N/m).

The electro-hydraulic proportional valve is simplified as a proportional link. The transfer function is

$$G_{sv}(s) = K_v = \frac{x_{vw}}{U} \tag{12}$$

where, x_{vw} is the displacement of the electro-hydraulic proportional valve spool (m), U is the input voltage of the electro-hydraulic proportional valve (V), K_v is the proportional gain of the electro-hydraulic proportional valve(m/V).

The position sensor is equivalent to a proportional link whose transfer function can be expressed as

$$K_f = \frac{U_f}{y_w} \tag{13}$$

where, K_f is the proportional gain of the position sensor (V/m), U_f is the output voltage of the position sensor feedback(V).

A nonlinear model of the bending control system's output displacement can be established by using the Laplace transform of Eqs(6), (10), and (11) combining Eqs(12) and (13). The block diagram of the bending cylinder control system is shown in Fig. 6.

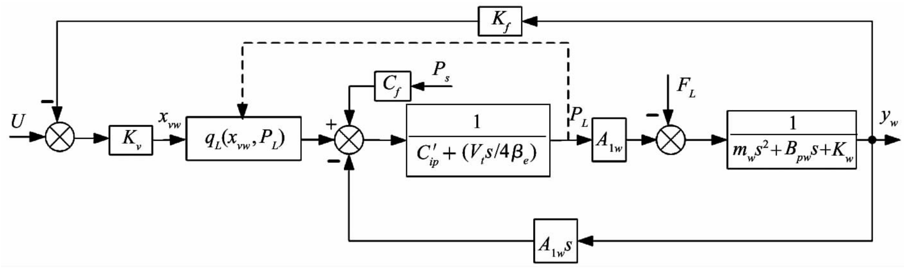

Fig. 6 Bending control system block diagram 3 coordination control strategy

The essence of upsetting-bending stroke coordination control is a tracking problem of position closed loop system. Only using PID controller to improve tracking property of bending control system is unable to meet the requirement of upsetting and bending coordination control. When the position of the cylinder is changed due to load variation or nonlinear factors, a predictive feed-forward link is introduced into the control system. The control quantity of velocity feed-forward can be used as the main compensation signal. The gain of PID can assist the velocity forward link to complete the final adjustment, which can improve the response and position accuracy of the system. The block diagram of the coordination control principle is shown in Fig. 7.

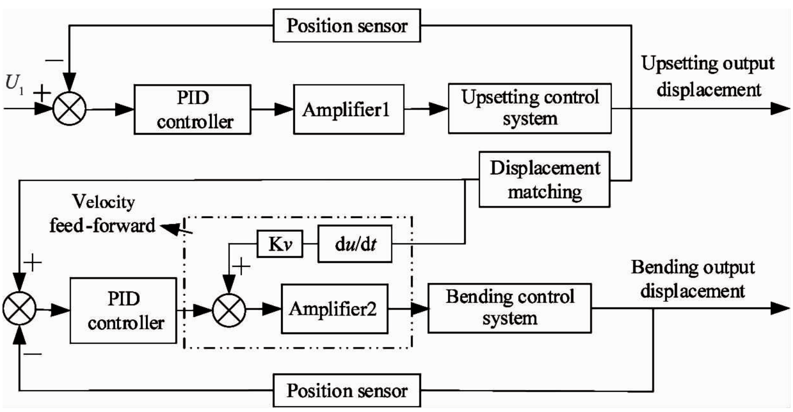

Fig. 7 Block diagram of master-slave coordination control based on velocity feed-forward

According to the upsetting-bending coordination motion curve in Fig. 2, the output displacement of the upsetting control system after the displacement matching in Fig. 7 is input to the bending control system as an input signal of the bending system.

As shown in Fig. 2, the displacement matching is divided into 3 stages. Assuming that the upsetting cylinder moves at a uniform velocity, the displacement of the bending cylinder is calculated according to the upsetting-bending process. The specific expression is shown as Eq. (14).

$$r_w = \begin{cases} \int_0^t (\frac{\mathrm{d}x}{\mathrm{d}t} \times 0.67)\mathrm{d}t & 0 < t \leqslant t_1 \\ \int_0^t (\frac{\mathrm{d}x}{\mathrm{d}t} \times 0.67)\mathrm{d}t & t_1 < t \leqslant t_2 \\ \int_0^t (\frac{\mathrm{d}x}{\mathrm{d}t} \times 0.67)\mathrm{d}t + \int_{t_2}^{t_3} (\frac{\mathrm{d}x}{\mathrm{d}t} \times 1.18)\mathrm{d}t & t_2 < t \leqslant t_3 \end{cases} \tag{14}$$

where, r_w is the input displacement of the bending cylinder after displacement matching, x is the output displacement of the upsetting control system, t is working time.

According to Eq. (14), a logic control solver using a velocity signal is constructed as shown in Fig. 8 for the logic control part of the upper computer of the experimental system.

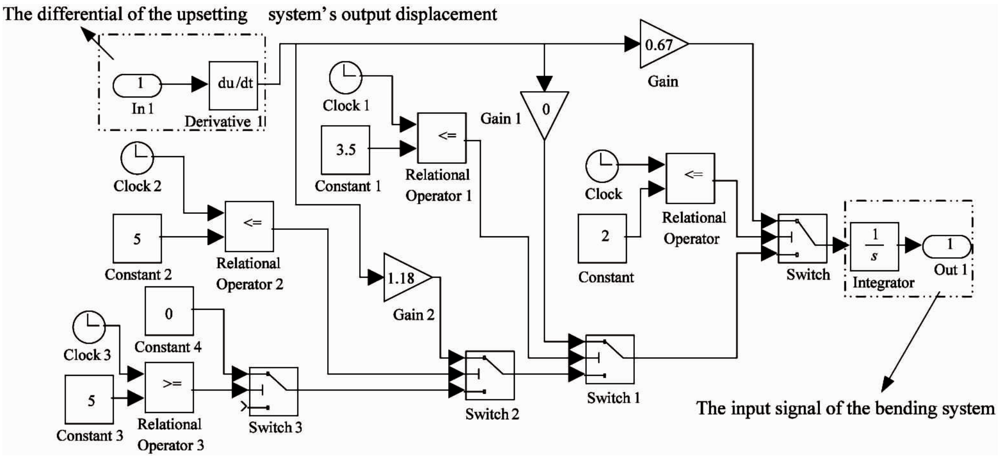

Fig. 8 Logic control program of displacement matching link

3 Experiment and discussion

3.1 Experiment rig

In order to further verify the feasibility of the coordination control strategy proposed in this paper, an experiment rig simulating the upsetting-bending coordination control principle is built.

The coordination control experiment rig shown in Fig. 9 consists of 2 sets of servo valve control cylinders, all of which are closed-loop position control system. The working principle of the position closed loop system is to collect the instantaneous position of each hydraulic cylinder through its own position sensor, to convert it into a difference between its voltage signal and the given voltage signal, to obtain respective deviation signal to control the flow of the respective servo valve to further control the position of the 2 hydraulic cylinders. In particular, the displacement signal of the upsetting cylinder after the displacement matching is input to the bending system, as shown in Fig. 7.

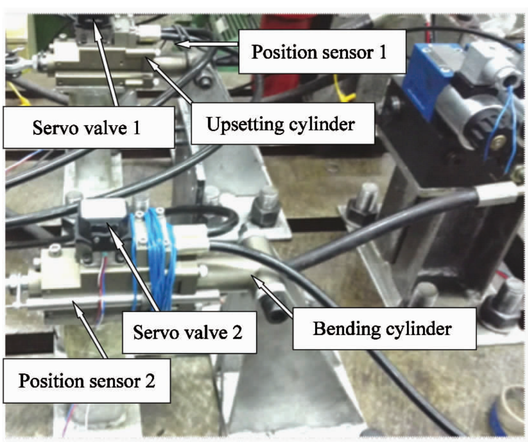

Fig. 9 Coordination control experiment rig

The schematic diagram of the coordination control experiment rig is shown in Fig. 10. The relief valve 4 is used to regulate the system pressure. Accumulator 7 is used to stabilize oil supply pressure of the servo valve. Reversing valve 13 is used to open and close the oil circuit.

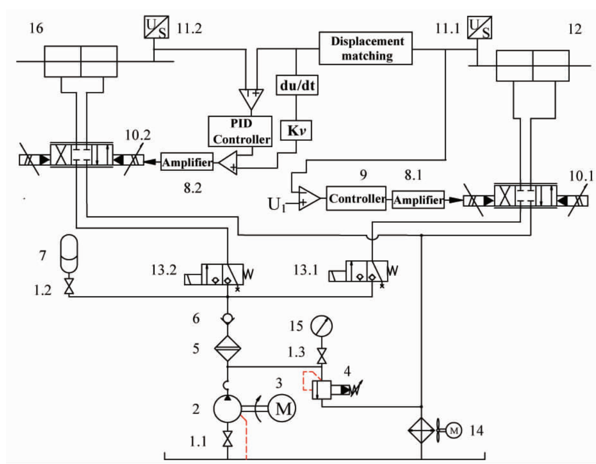

1 Shut-off valve, 2 Fixed displacement pump, 3 Electric motor, 4 Relief valve, 5 High-precision filter, 6 Check valve, 7 Accumulator, 8 Amplifier, 9 Controller, 10 Electro-hydraulic servo valve, 11 Position sensor, 12 Upsetting cylinder, 13 Directional valve, 14 Cooler, 15 Pressure gauge, 16 Bending cylinder

Fig. 10 The schematic diagram of the coordination control experiment rig

The parameters of the main components are listed in Table 1.

Table 1 Parameters of experiment rig

Name	Value	Unit
Servo valve flow (Δp = 7 MPa)	7	L/min
Step response time of servo valve	4	ms
Servo valve bandwidth (25% of input signal)	120	Hz
Position sensor stroke	± 25	mm
Position sensor accuracy	0.5	%
Pump displacement	25	ml/r
Pump rated speed	1 500	r/min
Working pressure	25	MPa

The controller uses a German semi-physical simulation platform dSPACE, and the DS1104 control board has 8 analog inputs and outputs, 20 digital inputs and outputs, and 2-channel encoder measures. However, the Matlab/Simulink control system model can be compiled to generate executable codes and downloaded to the DS1104PPC controller board using RTI. The real-time control interface can be realized using ControlDesk software provided by dSPACE, which can realize the real-time output of the system control quantity and on-line acquisition of the experimental data.

3.2 Coordination control strategy verification

In order to verify the correctness of the master-slave PID coordination control strategy based on the velocity feed-forward, the follow error of both the PID controller and the master-slave PID coordination control strategy based on the velocity feed-forward is compared.

The coordination experiment curve under PID control is shown in Fig. 11. The coordination experiment curve under master-slave PID control based on velocity feed-forward is shown in Fig. 12.

As shown in Fig. 11 (a), Fig. 11 (b) and Fig. 12(a), Fig. 12(b), it is known that when the upsetting cylinder is input to the slope signal, the output displacement signal of the upsetting cylinder is matched and then input to the bending cylinder to achieve the coordination motion.

The velocity curves of the upsetting and bending cylinders in Fig. 11(c) and Fig. 12(c) show that the input signal of the bending cylinder is divided into 3 stages. The displacement matching of Fig. 2 is realized.

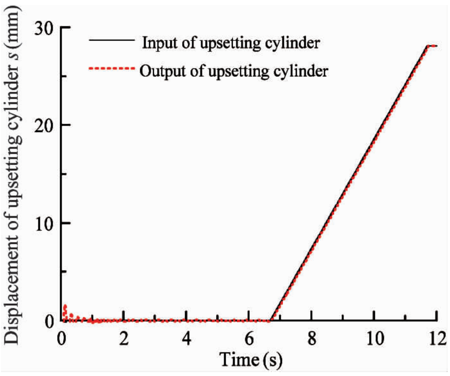

(a) Motion curve of upsetting cylinder

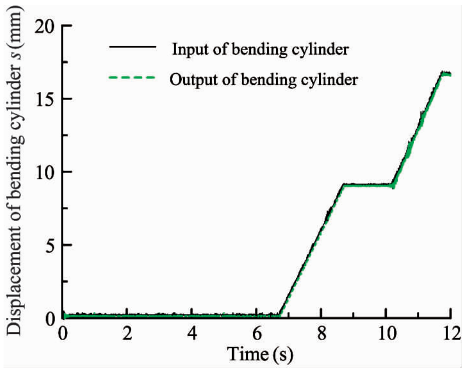

(b) The coordination motion curve of bending cylinder

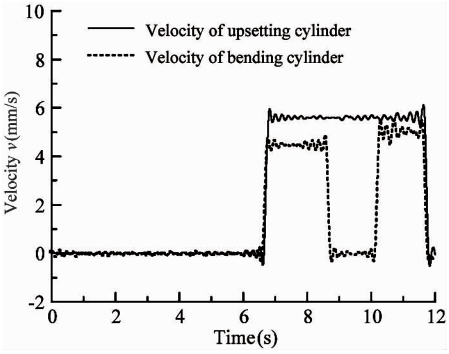

(c) Velocity curves of upsetting and bending cylinders

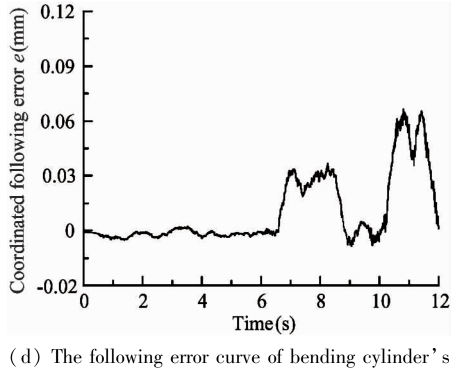

(d) The following error curve of bending cylinder's the coordination motion

Fig. 11 Coordination experiment curve under PID control

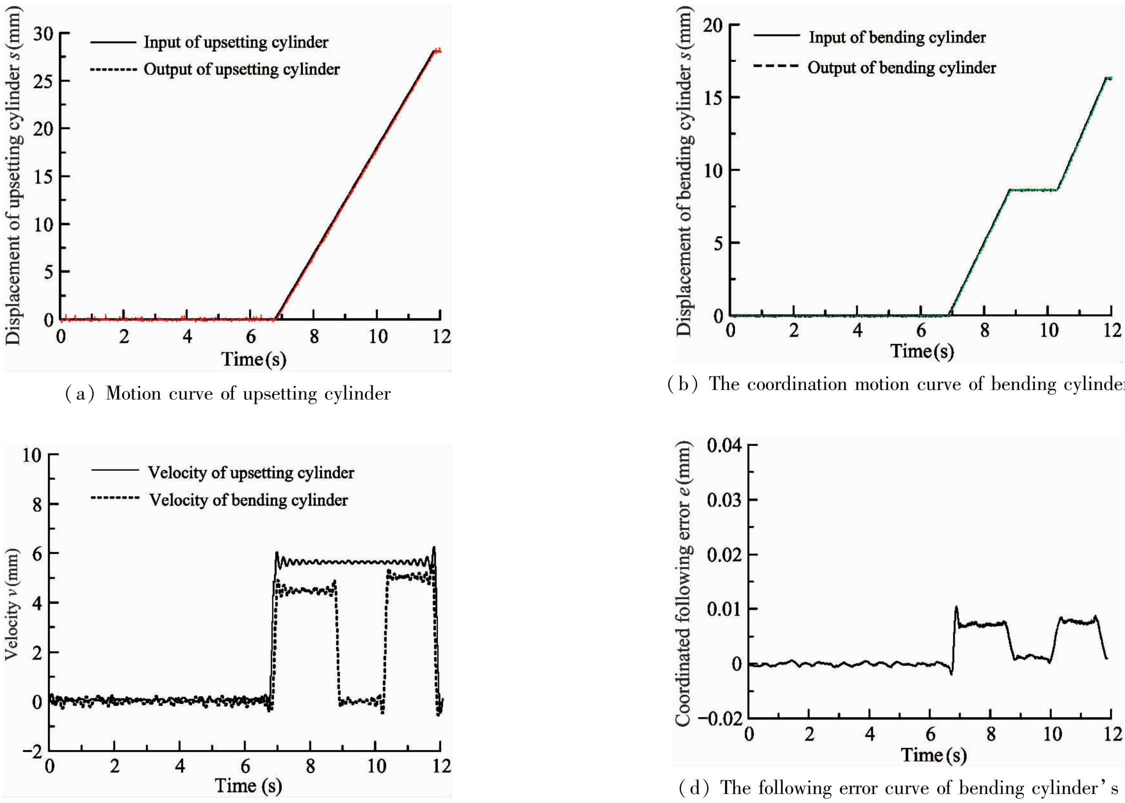

(a) Motion curve of upsetting cylinder

(b) The coordination motion curve of bending cylinder

(c) Velocity curves of upsetting and bending cylinders

(d) The following error curve of bending cylinder's the coordination motion

Fig. 12 Coordination experiment curve under master-slave PID control based on velocity feed-forward

As shown in Fig. 11(d) and Fig. 12(d), the following error of the bending cylinder increases gradually in the first stage under the PID controller. The maximum following error value is 0.031 mm. The maximum following error value of the master-slave PID control strategy based on the velocity feed-forward is 0.01 mm.

In the second stage, the bending cylinder stops moving. The displacement of the bending cylinder with the PID controller is fluctuant. The second stage following error is close to zero and has no fluctuation with the master-slave PID control strategy based on the velocity feed-forward.

In the third stage, the bending cylinder has the largest velocity. Under the PID controller, the following error increases. The maximum value is 0.06 mm. However, the following error with the master-slave PID control strategy based on velocity feed-forward is basically the same as that of the first stage, with a maximum value of 0.01 mm.

It can be seen from the following error curve that, the following error fluctuates less in the master-slave PID control strategy based on the velocity feed-forward compared to the PID control. The coordination precision of the 2 hydraulic cylinders is higher, that is, the bending cylinder can better follow the output signal after the upsetting cylinder position matching. The master-slave PID control strategy based on velocity feed-forward can reduce the following error of coordination motion effectively.

4 Conclusion

The mathematical model of the upsetting and bending system based on the crankshaft forging hydraulic press is set up. The master-slave PID coordination control strategy based on velocity feed-forward is constructed. The coordination control experiment rig is built to test the above control strategy. The experimental results show that the maximum following error value of the master-slave PID control strategy based on the velocity feed-forward is 0.01 mm and the second stage following error has no fluctuation. The maximum tracking error of the coordination control strategy is reduced by 66% compared with the traditional PID controller. The precision of the coordination motion is improved effectively under the control strategy.

References

[1] Xu S S, Ren Y L, Qi Z Y. Technique development of forming the marine crankshaft forgings[J]. *Heavy Casting and Forging*, 2018(1):19-22

[2] Wan X Y. The exploration of the forging method for the

large-middle size continuous grain flow crankshaft[J]. *Heavy Casting and Forging*, 2006(3):45-52

[3] Zhang X Z, He W W, Liu J S, et al. Development of the bending and upsetting forging method for the integral crankshaft[J]. *Mechanical Engineering & Automation*, 2008(6):198-200

[4] Cui H X, Zhang D K, Zhou J J, et al. The special hydraulic press for upsetting and bending of crankshaft[P]. China Patent: CN1836804, 2006 (In Chinese)

[5] Cui H X, Duan Z G, Zhang Z C. "NTR" method of bending and upsetting technology for all fiber crankshafts [J]. *Journal of Machine Design*, 2006(6): 151-152

[6] Chen T S. Comparative Analysis and Research of RR, TR and NTR Upset-bending Processes for Heavy Crankshaft of Continuous Grain flow[D]. Tianjin: Tianjin University, 2005: 1-10 (In Chinese)

[7] Jin M. Study on bending and upsetting forging 305 marine crankshaft[J]. *Advanced Materials Research*, 2010, 97 (6): 337-343

[8] Peng X B, Gong G F, Chen K, et al. Synchronization fuzzy PID control of lifting hydraulic cylinders for segment erector[J]. *Journal of Zhejiang University (Engineering Science)*, 2014, 48(11): 2002-2008

[9] Liu C F, Zhou L, Wu S L. Research on synchrony-technology of dual electro-hydraulic servo system based on decoupling control[J]. *Machine Tool & Hydraulics*, 2007, 35(2): 181-184

[10] Mochizuki K, Motai T. Synchronization of two motion control axes under adaptive feedforward control[J]. *Journal of Dynamic Systems Measurement & Control*, 1992, 114(2):196-203

[11] Heinrichs, B N, Sepehri, A B. Thornton. Position-based mpedance control of an industrial hydraulic manipulator [J]. *IEEE Control System Magazine*, 1997, 17(1): 46-52

[12] Chen C Y, Liu L Q, Cheng C C, et al. Fuzzy controller design for synchronous motion in dural-cylinder electro-hydraulic system[J]. *Control Engineering Practice*, 2008 (16): 658-673

[13] Deng F, Su W B, Guo Q Y, et al. Intelligent control for electro-hydraulic position servo synchronic control system with double cylinders[J]. *Journal of Xi'an Jiaotong University*, 2011, 45(11): 85-89

[14] Wang H J. Application of quantitative feedback theory on synchronization controller design of dual actuators driven system[J]. *Cilliery Mechanical & Electrical Technology*, 2015(1): 68-70

[15] Liu Z W, Qing X Q. Research on fuzzy PID control for synchronization system of giant die forging hydraulic press [J]. *Forging & Stamping Technology*, 2015, 40(4): 89-92

[16] Shi S W, Zhang G H. Application of fuzzy control in the synchronization control system for a 10 000 t hydraulic press[J]. *Chinese Hydraulics & Pneumatics*, 2006(1): 28-30 (In Chinese)

[17] Li J Y, Yi M L, Wang Y, et al. High-accuracy synchronization control with hybrid neural networks[J]. *Chinese Journal of Mechanical Engineering*, 2005, 18(1): 127-131 (In Chinese)

Yao Jing, born in 1978. She received the B. S. in mechanical engineering from Yanshan University, Qinhuangdao, China in 2001, and M. S. and Ph. D degrees in mechatronics engineering from Yanshan University in 2004 and 2009 respectively. She is currently a professor of mechatronics engineering, Yanshan University, China. Her research interests include electro-hydraulic servo control and heavy machinery fluid transmission and control.